buildings

MDPI

Article

Influence of HPMC and VAE on the Properties of Geopolymer Mortar

Wenjun Ji [1], Pengfei Chen [2], Ying Lu [1], Zeyang Zhang [2], Baolong Shan [1], Sha Li [2,*], Mengyan Chi [1] and Haifeng Yu [2,*]

[1] China Construction First Group Decoration Co., Ltd., Beijing 100161, China
[2] School of Civil Engineering, Hebei University of Science and Technology, Shijiazhuang 050018, China
* Correspondence: v501we@hebust.edu.cn (S.L.); skipperyhf@hebust.edu.cn (H.Y.); Tel.: +86-18631170013 (S.L.)

Abstract

The delamination of building facades creates a critical demand for inorganic adhesive mortars with high long-term adhesion. Geopolymer (GP) represents an eco-friendly alternative to Portland cement (PC). However, the effect of polymer additives, commonly used in cement-based adhesive mortars, on GP mortar remains insufficiently studied. This study examines the effects of hydroxypropyl methylcellulose (HPMC) and vinyl acetate-ethylene (VAE) polymer on the workability, mechanical properties, durability, and microstructure of GP mortar. Results show that an optimal HPMC content (0.4 wt%) improves the fluidity, compressive strength, and adhesive strength of GP mortar, approximately 6%, 16%, and 20%, respectively. These enhancements are attributed to the incorporation of uniformly distributed microbubbles in the mortar matrix. Beyond this optimal content, however, HPMC impairs flowability and adhesion due to its thickening effect. In contrast, VAE addition significantly enhanced adhesive strength by approximately 28%, albeit at the cost of a 17% reduction in compressive strength, resulting from the retardation of the alkali activation process. This gain in adhesion is associated with the formation of a continuous polymer film that establishes both physical interlocking and chemical bonding with the GP matrix. Furthermore, HPMC improved the durability of the GP mortar, while VAE did not contribute to this aspect. These insights offer valuable guidance for designing high-performance GP-based adhesive mortars suitable for building applications.

Keywords: geopolymer; HPMC; VAE; adhesive strength; durability; microstructure analysis



Academic Editor: Geo Paul

Received: 9 September 2025
Revised: 1 October 2025
Accepted: 4 October 2025
Published: 9 October 2025

Citation: Ji, W.; Chen, P.; Lu, Y.; Zhang, Z.; Shan, B.; Li, S.; Chi, M.; Yu, H. Influence of HPMC and VAE on the Properties of Geopolymer Mortar. *Buildings* **2025**, *15*, 3621. https://doi.org/10.3390/buildings15193621

Copyright: © 2025 by the authors. Licensee MDPI, Basel, Switzerland. This article is an open access article distributed under the terms and conditions of the Creative Commons Attribution (CC BY) license (https://creativecommons.org/licenses/by/4.0/).

1. Introduction

The delamination of building facades is a common problem in construction. The insufficient adhesive strength of the mortar connecting the structural and decorative layers is one of the main causes of this problem. Most existing adhesive mortars are formulated by mixing organic glue with cement mortar. However, these materials suffer from high carbon emissions, are prone to degradation, and exhibit insufficient water and corrosion resistance. Therefore, it is important to develop inorganic adhesive mortars with low-carbon emissions, high adhesion, and high durability.

Geopolymer (GP) is inorganic material with properties comparable to those of organic polymers [1]. It offers advantages such as recyclability, high adhesive strength, and excellent resistance to acid, alkali, and high temperatures [2]. Existing studies have found that the GP matrix contains minimal high-calcium minerals such as tricalcium silicate. Instead, it undergoes alkali activation and polycondensation reactions, ultimately generating a large number of spatially reticulated C-(A)-S-H and N-A-S-H gels [3]. Compared to the

substantial calcium hydroxide (CH) initially produced by cement hydration, these gels are more likely to form a dense interfacial transition zone with aggregates or existing substrates [4]. The alkali activators contained in GP mortar can also react with the Al and Si reactive components in the interfaces of old mortars to further enhance the adhesive properties of the interfacial transition zones [5,6]. Therefore, utilizing solid waste through alkali activation technology to develop environmentally friendly adhesive mortars with high durability is feasible. This approach offers a promising solution to the problem of facade delamination.

Cellulose ether (CE) and dispersible latex powder (VAE) are indispensable additives in existing adhesive mortars. CE is a class of polymeric compounds with an ether structure. Studies show that CE adsorbs onto cement particle surfaces, significantly enhancing the water retention of cement-based materials [7,8] and improving the adhesion and crack resistance of mortar [9]. The inhibitory effect of CE on C-S-H gel formation via molecular adsorption is stronger than its effect on C_3S mineral dissolution. The ether bonds can form coordination bonds with Ca^{2+} on C-S-H surfaces. This not only alters the morphology of hydration products but also inhibits ion migration through steric hindrance, thereby delaying the hydration exotherm peak [10,11]. However, CE addition increases porosity, particularly the volume of large pores, and alters pore shape and distribution. This leads to a more significant reduction in compressive strength than in flexural strength. A comparative study of CE types indicated that hydroxypropyl methylcellulose (HPMC) most effectively improves mortar adhesion [12]. When CE molecules contain methyl groups, their surface activity is higher, but their incorporation leads to a reduction in mortar strength [8]. The porosity caused by the addition of HPMC, on the other hand, helps to reduce the weight of the material, improve its thermal performance, and reduce energy consumption in construction [13].

VAE consists of polymer particles with a core-shell structure based on an ethylene-vinyl acetate copolymer, and it exhibits excellent film-forming and adhesive properties [14]. The polymer film generated by VAE can effectively fill and seal the pores, enhance the impermeability, and reduce the drying shrinkage [15,16]. The appropriate amount of VAE can significantly improve the adhesive strength, shear strength and tensile strength of cement-based mortar [14,17], raise the flexibility and extensibility of rubber mortar [18]. The incorporation of VAE, however, introduces entrapped air bubbles into the system [19]. An inhomogeneous distribution of these bubbles can disrupt the integrity of the pore structure, resulting in reduced compressive strength [20,21] and diminished long-term durability [22]. In contrast, several studies have reported that VAE addition does not necessarily increase overall porosity. Instead, the observed strength reduction has been attributed to its inhibitory effect on the hydration process [23].

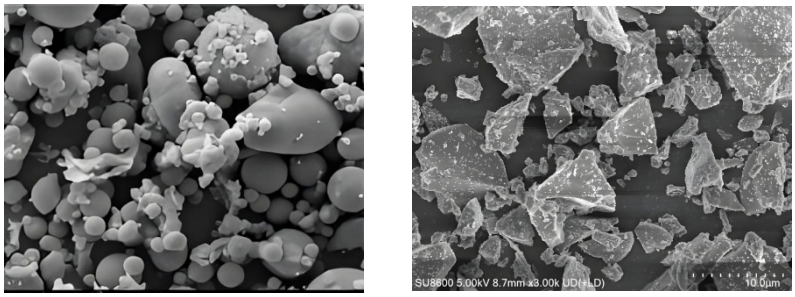
In summary, HPMC and VAE are effective in improving the bond performance of cement-based mortars. However, their effects and mechanisms on GP mortar remain unclear. To enhance the durability of GP mortar, it is essential to elucidate the modification mechanisms of HPMC and VAE. Based on this, this paper systematically investigates the modification mechanisms of HPMC and VAE on the workability, mechanical properties, and durability of GP mortar. It is of great significance to promote the high value-added utilization of solid waste, improve durability and reduce the cost and carbon emission of adhesive mortar.

2. Materials and Experiments

2.1. Materials

Grade-II Class F fly ash (FA) was obtained from Hebei Kexu Building Materials Co. (Lingshou County, Shijiazhuang City, Hebei Province, China), Ltd. Granulated blast-furnace

slag (GBFS), classified as high-quality and highly reactive according to GB/T 203-2008, was sourced from Jinghang Mineral Products Co., Ltd. (Lingshou County, Shijiazhuang City, Hebei Province, China). Figure 1 and Table 1 present the scanning electron microscopy (SEM) micrographs and chemical compositions of these binders, respectively.



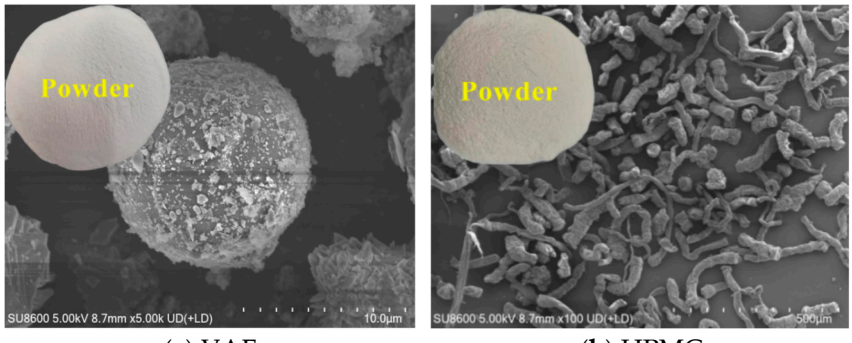
(**a**) Fly ash powder (**b**) BFS powder

Figure 1. SEM micrographs for raw binder materials.

Table 1. Chemical compositions of the binder materials.

Oxide (wt.%)	SiO_2	Al_2O_3	CaO	Fe_2O_3	TiO_2	SO_3	K_2O	MgO	Others
FA	50.56	37.23	2.40	5.21	1.54	1.05	1.00	0.21	0.8
BFS	31.10	15.68	41.75	0.46	1.42	3.24	0.28	5.18	0.89

The vinyl acetate-ethylene (VAE) copolymer was supplied by Langfang Tianya Energy-Saving Technology Co., Ltd. (Langfang City, Hebei Province, China), with glass transition temperature (Tg) less than 5 °C. Hydroxypropyl methylcellulose (HPMC) was obtained from Chuangsheng Building Materials Chemical Co., Ltd. (Shijiazhuang City, Hebei Province, China), exhibiting the carbonization and discoloration temperatures of 280–300 °C and 190–200 °C, respectively. The viscosity of HPMC provided by the manufacturer is 193,000/mpa·s (4.0% at 20 °C). As shown in Figure 2, VAE particles are spheroidal, whereas HPMC adopts a chain-like morphology. Their chemical compositions are listed in Table 2.



(**a**) VAE (**b**) HPMC

Figure 2. SEM micrographs for VAE and HPMC.

Table 2. Chemical compositions of VAE and HPMC.

Oxide (wt.%)	SiO_2	CaO	MgO	Na_2O	Al_2O_3	Fe_2O_3	SO_3	Cl	Others
VAE	44.42	33.18	16.29	2.67	-	1.15	0.61	0.42	1.26
HPMC	2.38	4.24	-	15.96	1.34	0.69	20.90	54.36	0.13

The fine aggregate was Zhengding River sand, with a mud content below 1%, a moisture content below 0.3%, and a fineness modulus of 2.63 after screening and grading, classifying it as medium sand with continuous grading in Zone II.

Alkali activated solution (AAS) was prepared by mixing sodium hydroxide and water glass. The sodium hydroxide (NaOH), with a purity of ≥99% and a pH greater than 14, was obtained from Longbang Chemical (Cangzhou City, Hebei Province, China). Water glass was produced from Bengbu Jingcheng Chemical Co., Ltd. (Bengbu City, Anhui Province, China), with a pH of 11.3 and a solid content of 34.8%. Both the NaOH solution (10 mol/L) and the water glass solution needed to be prepared one day before the experiment. The water glass solution was prepared by diluting industrial-grade water glass with water in a volume ratio of 1:1. Both this and the NaOH solution (10 mol/L) were prepared one day in advance. Then the two solutions were mixed in proportion according to the experimental design. The water used was tap water.

2.2. Experimental Design

Based on previous research and practical application requirements [24], seven mixture proportions were designed, as detailed in Table 3. This study systematically investigated the effects of HPMC and VAE dosage on the workability, mechanical properties (compressive, flexural, split tensile, and adhesive strength), and durability of geopolymer (GP) mortar.

Table 3. Mixture proportions of GP mortar samples (Weight ratio to binders (BFS + FA)).

Factors	Series	Binders		River Sand	WG: NH	AAS/Binders	Admixtures (wt.,%)	
		FA	BFS				HPMC	VAE
Reference	0	0.5	0.5	2	3:1	0.5	0	0
HPMC	X0.2	0.5	0.5	2	3:1	0.5	0.2%	0
	X0.4	0.5	0.5	2	3:1	0.5	0.4%	0
	X0.6	0.5	0.5	2	3:1	0.5	0.6%	0
VAE	V2	0.5	0.5	2	3:1	0.5	0	2%
	V4	0.5	0.5	2	3:1	0.5	0	4%
	V6	0.5	0.5	2	3:1	0.5	0	6%

Considering the significant influence of environmental conditions on the service life of adhesive mortars, three curing regimes were designed: standard curing (E1, T ≈ 20 °C, RH ≥ 90%), natural curing (E2, T = 15–25 °C, RH = 30–55%), and sealed natural curing (E3, T and RH were same to E2, double layer sealing of cling film). These regimes were used to investigate the effect of the curing environment on the mechanical properties of the GP mortar. Furthermore, the durability of the GP adhesive mortars was evaluated under three aggressive environments: water immersion, sulfate attack, and high temperature.

2.3. Experimental Method and Process

The preparation process for the GP adhesive mortar is illustrated in Figure 3. Specimens were demolded after 24 h and subsequently cured under the designated conditions until the testing age.

After 28 days of standard curing, cement mortar blocks (4 cm × 4 cm × 16 cm) were cut into 4 cm × 4 cm × 2 cm substrates using a cutting machine. To reduce errors in the tensile adhesive strength tests, 2-mm-deep grooves were made on the bonding surface of the cement substrates. A custom-fabricated apparatus (Figure 4) was used for this purpose. After casting the fresh GP mortar, the grooved cement substrates were placed on its surface to form the adhesive strength specimens (According to JC/T 547-2017 [25], with the size of the substrate changed from 50 mm to 40 mm). These specimens were then stored in different curing environments until the designated testing ages.

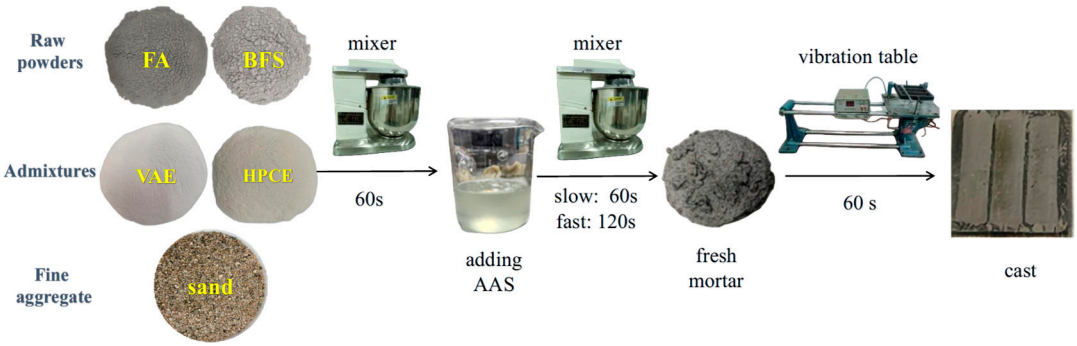


Figure 3. Preparation process of GP adhesive mortar.

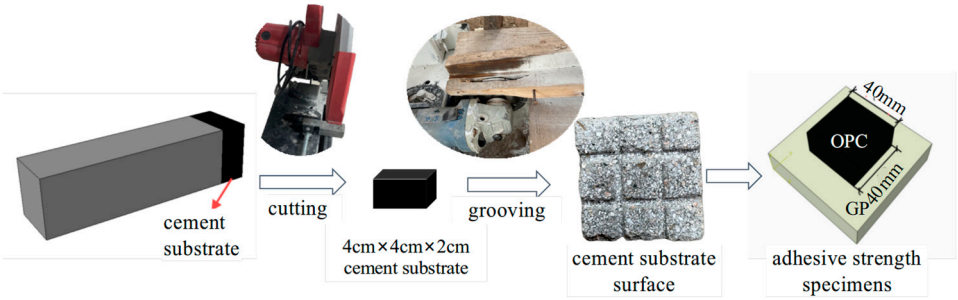


Figure 4. Preparation of the adhesive strength specimens.

The setting time and fluidity of the GP mortars were determined by following the standard test methods specified in GB/T 1346-2024 [26] and GB/T 2419-2005 [27], respectively. Flexural and compressive strengths were referred to GB/T 17671-2021 [28]. The split tensile strength was determined following GB/T 29417-2012 [29]. The Adhesive strength was tested with reference to JGJ/T 70-2009 [30] and JC/T 547-2017 [25]. The adhesive strength tests on the GP mortar–cement matrix specimens were conducted at different ages using the apparatus shown in Figure 5.



Figure 5. Adhesive strength apparatus.

The resistance to water, acid, and high temperature of the GP mortars was evaluated after 28 days of curing. For the water resistance test, specimens were immersed in a water tank located in the standard curing room. The water level was maintained at least 2 cm above the top of the specimens throughout the 14-day soaking period. Subsequently, the specimens were removed, surface water was wiped off, and they were left at room temperature for one hour before strength testing.

The sulfate corrosion experiment was conducted according to GB/T50082-2024 [31], as shown in Figure 6. Thermal aging experiment was carried out according to JC/T 547-2017 [25]. Based on existing results indicating that exterior wall temperatures can reach 88.6 °C in

summer [32], the thermal cycle was set between 20 °C and 80 °C. After 14 days of thermal cycling, the mechanical properties of the GP mortar were measured.



Figure 6. Sulfate corrosion experiment process.

In order to clearly characterize the effects of water immersion, sulfate attack, and high temperature on the mechanical properties of GP mortars, the corrosion resistance coefficient K_{ij} was introduced to characterize the resistance of GP mortars to the environments, as shown below:

$$K_{ij} = \frac{f_{jn}}{f_{j0}} \quad (1)$$

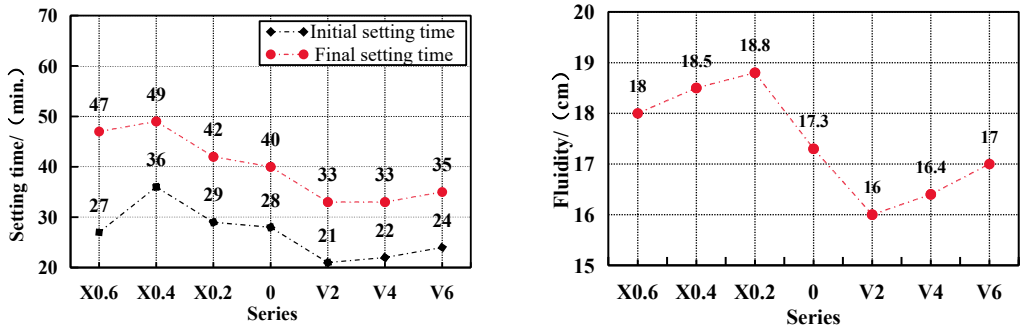
where: K_i—corrosion resistance coefficient (%); f_{j0}—the strength before erosion, MPa; f_{jn}—the strength after erosion, MPa; "$i = w$"—immersion in water; "$i = s$"—sulfate attack; "$i = T$"—high temperature; f_c ($j = c$)—compressive strength; f_{cf} ($j = cf$)—flexural strength; f_t ($j = t$)—tensile strength; f_a ($j = a$)—adhesive strength.

X-ray diffraction (XRD) analysis was carried out using a SmartLab 9KW X-ray diffractometer manufactured by Rigaku Corporation of Japan, with a scanning speed of 5°/min, a step size of 0.02°, and a scanning range of 5° to 100°. Scanning electron microscope (SEM) test was conducted by HITACHI, Tokyo, Japan, focusing on the analysis of the microstructure at the interface between the adhesive mortar and the substrate.

3. Results and Analysis

3.1. Workability

The effects of HPMC and VAE dosage on the workability of GP mortar are shown in Figure 7. As shown in Figure 7a, the initial and final setting times of the GP mortar initially increased and then decreased as the HPMC dosage increased. When 0.4% of HPMC was added, the initial and final setting times were extended by 28.6% and 22.5%, respectively. This indicates that the addition of appropriate HPMC can prolong the initial and final setting time of GP mortar. The effect of VAE on the setting times showed an opposite trend, first shortening and then slightly increasing. At low dosages, the thickening effect of VAE was more pronounced, leading to shorter setting times. However, at higher dosages, VAE's moisture-retaining ability increased, which prolonged the hydration reaction and consequently increased the setting time [33].



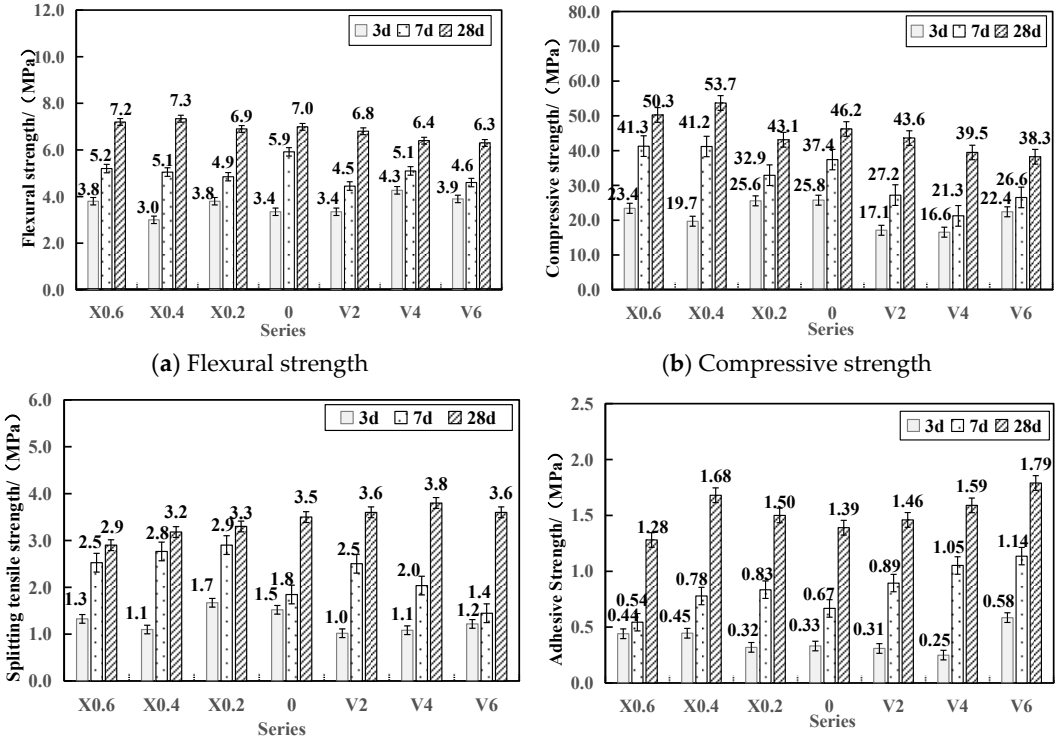
(**a**) Setting time (**b**) Fluidity

Figure 7. Workability of GP mortars.

The fluidity of the GP mortar first increased and then decreased with higher HPMC dosage, peaking at a dosage of 0.2% (a 4.1% increase over the baseline group). This is mainly due to the high water retention of cellulose ether, which helps water to form a water film between mortar particles, reduces the frictional resistance between solid particles, and increases the inter-slurry fluidity. However, too much HPMC will adsorb free water through hydrogen bonding, increasing the viscosity of the slurry and leading to a decrease in flowability. The influence of VAE on fluidity followed a pattern similar to its effect on setting time. At a 2% dosage, VAE absorbed water, causing a significant decrease in fluidity. However, at higher dosages, the film-forming and lubricating properties of VAE became dominant [34], leading to an improvement in fluidity.

3.2. Mechanical Strength

By comparing the mechanical properties of GP mortars with different dosages of HPMC and VAE, as shown in Figure 8, it was found that with the increase of HPMC dosage, the flexural strength of GP mortar showed a slight upward trend overall, the compressive strength value first increased and then slightly decreased, and the 28 day tensile strength gradually decreased. However, the 7-day tensile strength of GP mortar mixed with HPMC was higher than that of the reference group. The adhesive strength showed a trend of first increasing and then decreasing. However, excessive HPMC dosage led to the formation of air bubbles due to its air-entraining effect, which reduced the compactness and homogeneity of the mortar, thereby weakening its strength [35].



(**a**) Flexural strength (**b**) Compressive strength

(**c**) Tensile Strength (**d**) Adhesive strength

Figure 8. Mechanical properties of GP mortar specimens at different curing ages.

The addition of VAE was detrimental to the flexural and compressive strength of GP mortar. With the increase of VAE content, the flexural and compressive strength decreased. However, it slightly improved the tensile strength and significantly enhanced the adhesive strength. At a VAE content of 6%, the 28-day adhesive strength reached 1.79 MPa, which exceeds the minimum requirement of 0.6 MPa specified in the JG/T 287-2013 standard [36]. The mechanism involves the synchronization of the VAE film-forming process with the GP mortar hydration [37]. The

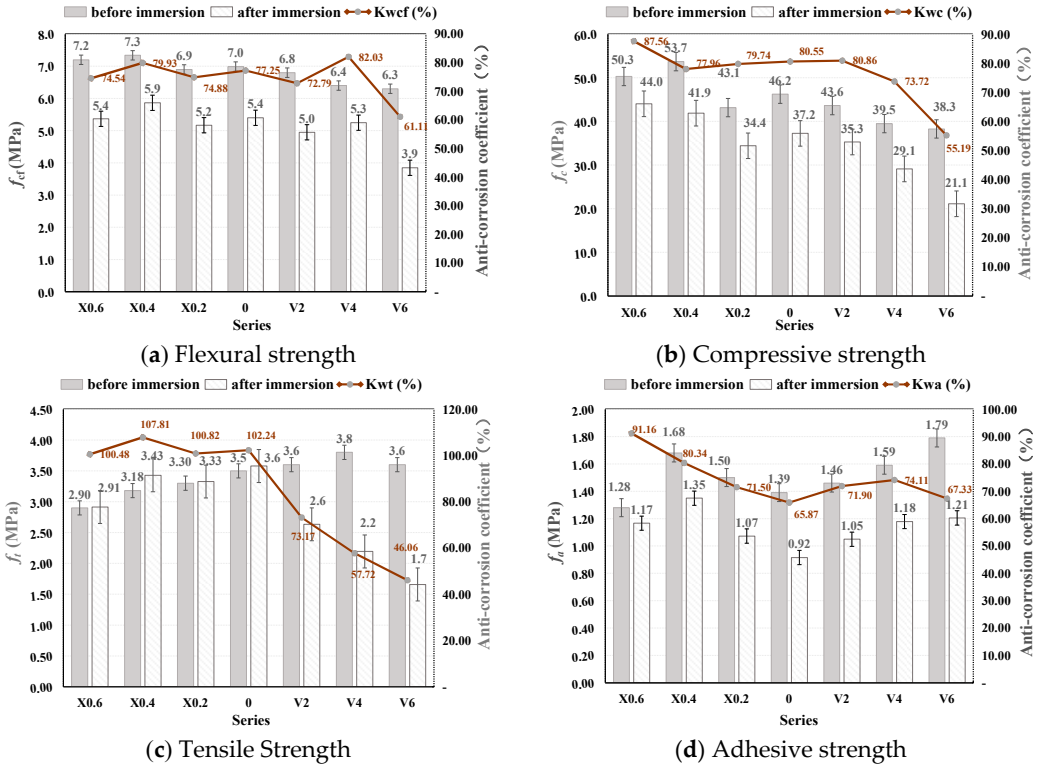
amount of polymer film formed increases with VAE content, thereby enhancing the adhesive and tensile strengths. However, the water absorption of VAE may delay the hydration reaction process, leading to incomplete reaction of the cementitious material and resulting in a decrease in the flexural and compressive strength of GP mortar [20,38]. The effect of VAE on the strength of GP mortar is similar to that of VAE on the strength of cement-based mortar. The optimal dosage of VAE can enhance interfacial bonding and flexural strength, while excessive use can increase porosity and delay the hydration reaction process [23].

3.3. Durability

The Chinese regulations clearly stipulate the adhesive strength limits of adhesive mortar before and after immersion in water. Therefore, the changes in the mechanical properties of seven GP mortar mixes before and after water immersion were compared. Additionally, the high-temperature aging resistance and sulfate corrosion resistance of the GP adhesive mortar were investigated.

3.3.1. Water Immersion

Figure 9 shows that after immersion, most mechanical properties of the GP mortars decreased, except for a slight increase in the tensile strength of the reference and HPMC groups. A comparison of the corrosion resistance coefficients before and after immersion revealed that the GP mortar with HPMC exhibited slightly higher coefficients than the reference group in flexural, compressive, and tensile strength. HPMC had a significant effect on improving the corrosion resistance coefficient for adhesive strength, which increased by over 25%. With the increase of VAE content, the adhesion strength-corrosion resistance coefficient of GP mortar showed a trend of first increasing and then decreasing. At a content of 4%, it increased by approximately 8%. However, the addition of VAE was detrimental to the flexural, compressive, and tensile strength of GP mortar after immersion. The decrease in the corrosion resistance coefficient for tensile strength was particularly significant. The microstructure changes of GP mortar shown in SEM images can precisely explain the above phenomenon.



(**a**) Flexural strength (**b**) Compressive strength

(**c**) Tensile Strength (**d**) Adhesive strength

Figure 9. Mechanical properties of GP mortar specimens before and after water immersion.

3.3.2. Sulphate Attack

To compare the effects of HPMC and VAE on sulfate and high-temperature resistance, the X0.4 and V6 series, which exhibited good adhesion in previous tests, were selected. These were compared with the reference group to evaluate the durability improvement offered by HPMC and VAE.

Figure 10 compares the changes in mechanical properties before and after sulfate attack for the X0.4, V6, and reference groups. It can be clearly seen that HPMC helps to improve the ability of GP mortar to resist sulfate attack, and the coefficients of various mechanical properties against sulfate attack are larger than those of the reference group, especially the enhancement effect on tensile strength. In contrast, the improvement effect of VAE was not ideal. The addition of VAE adversely affected the sulfate resistance for all mechanical properties except adhesive strength. This is related to its loose microstructure, which allows sulfate ions to penetrate the GP matrix more easily, leading to reduced resistance.

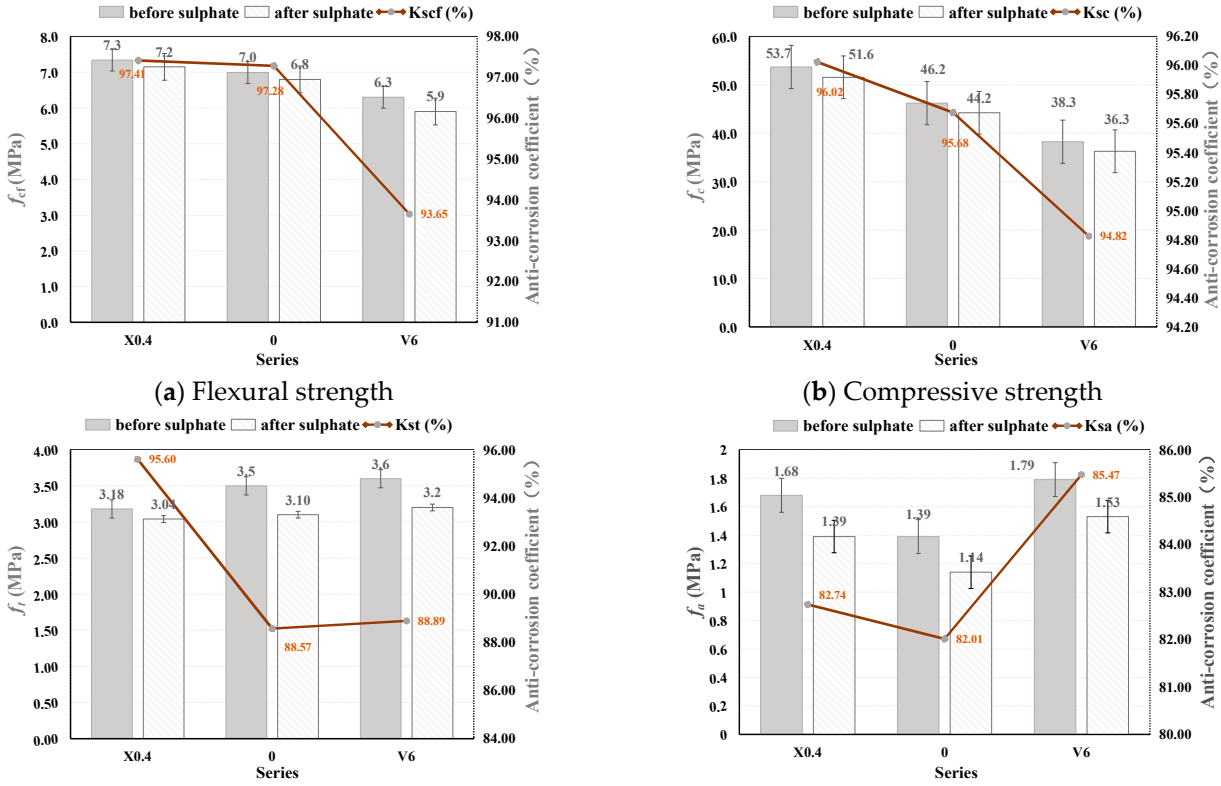


Figure 10. Mechanical properties of GP mortar specimens before and after sulphate attack.

3.3.3. High Temperature

The changes in the mechanical properties of X0.4, V6 and the reference group before and after high temperature cycling at 80–20 °C are shown in Figure 11. The addition of 0.4% HPMC did not significantly reduce the mechanical properties after high temperature exposure; instead, it increased the corrosion resistance coefficients for flexural and tensile strength by approximately 6%. These findings are consistent with the study by Batista et al., which reported that HPMC improves water retention and thermal insulation in rendering mortars, while also reducing bulk density due to increased porosity [13].

The addition of VAE significantly reduced the high-temperature resistance of GP mortar, especially for its flexural and adhesive strength. After high temperature, the corrosion resistance coefficient of flexural and adhesive strength decreased by about 24% and 13%, respectively. It is speculated that the above results are related to the structural

damage of VAE polymer film. Existing research has confirmed that the polymer film formed by VAE in cement mortar undergoes structural damage after a 70 °C heat aging test [39].

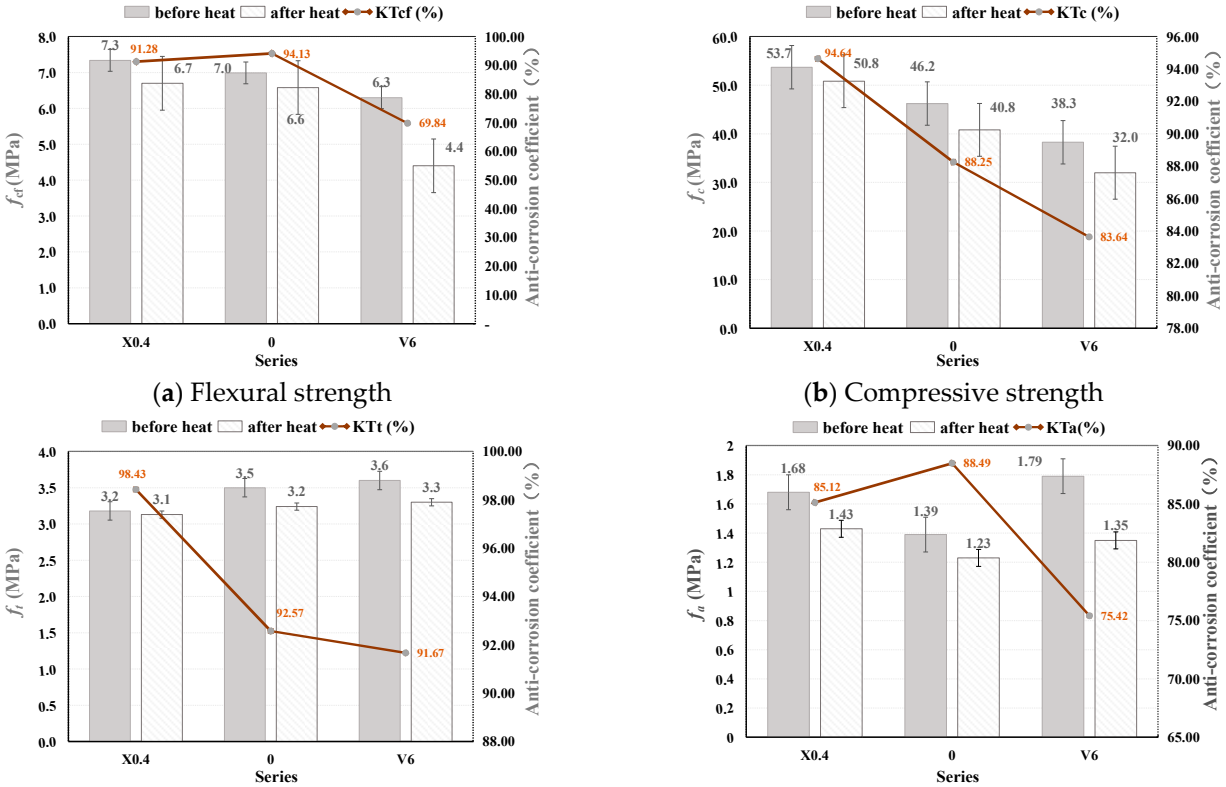


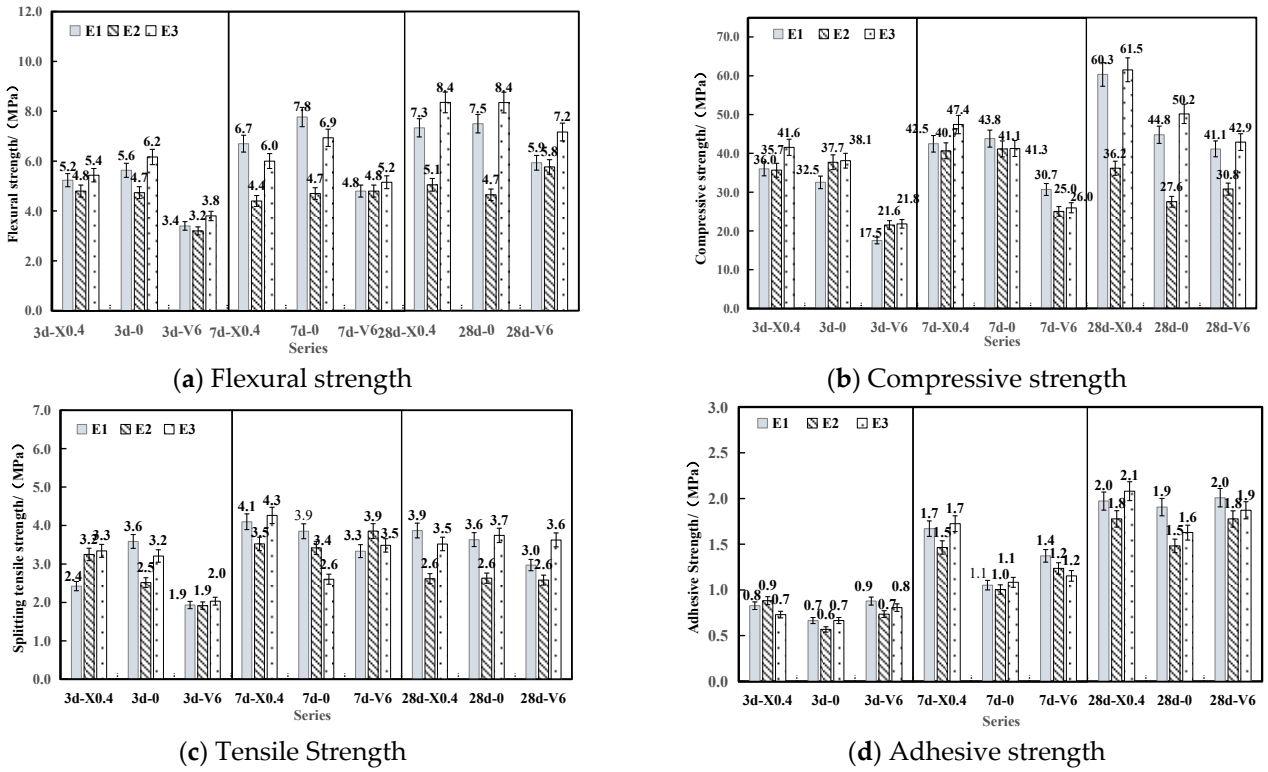
Figure 11. Mechanical properties of GP mortar specimens before and after high temperature.

3.3.4. Effect of Curing Conditions

Figure 12 shows the effects of three curing environments, E1 (standard curing), E2 (natural curing), and E3 (natural sealing curing), on the flexural, compressive, tensile, and adhesive strengths of the reference, X0.4, and V6 series at 3, 7, and 28 days. The results reveal that standard curing and natural sealing curing are more favorable for the development of mechanical properties in GP mortar. With increasing age, the natural sealing curing can equal or even exceed the standard curing. This is consistent with the results of the previous study [40]. It is impossible to achieve a standard curing environment during on-site construction. Therefore, the mechanical properties of GP mortar can be guaranteed by sealing during construction.

3.4. SEM Analysis

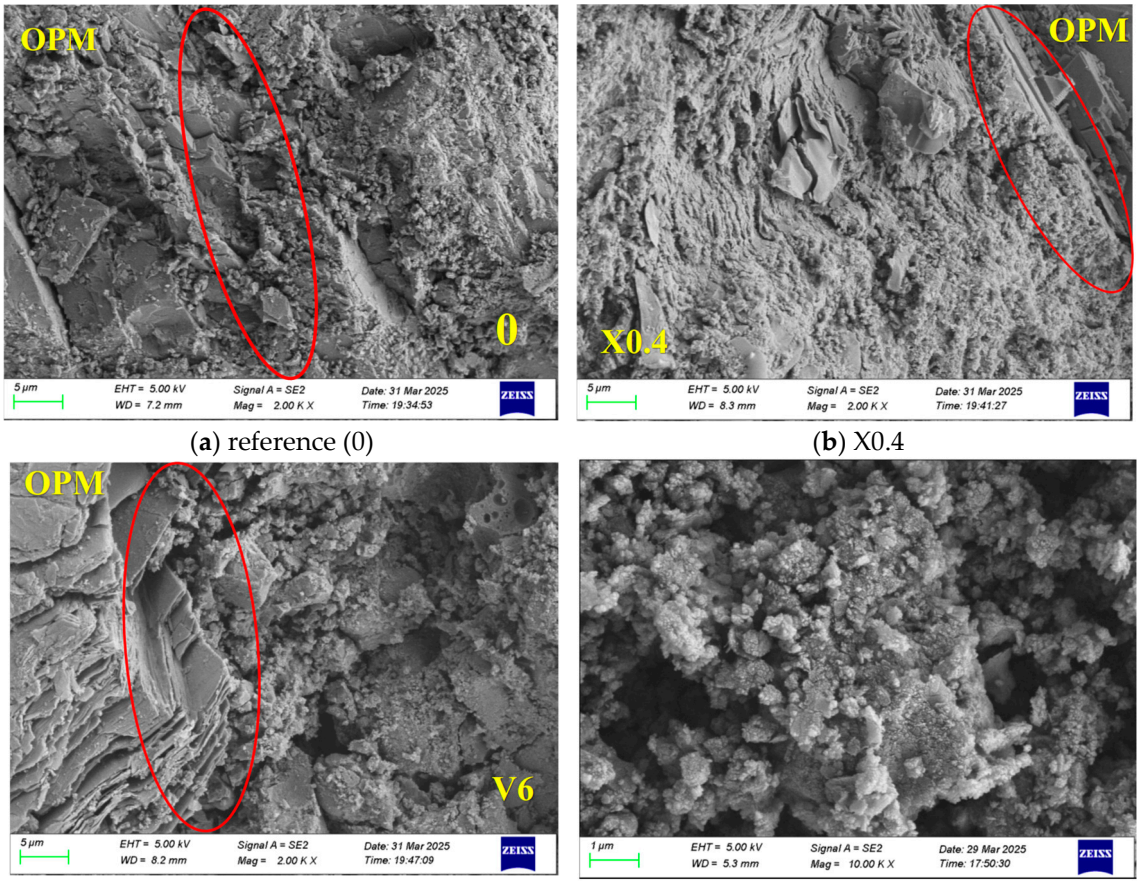
A comparison of the SEM micrographs for sample X0.4 (with 0.4% HPMC), sample V6 (with 6% VAE), and the reference group (Figure 13) reveals distinct microstructural features. The micrograph of the reference group, shown in Figure 13a, displays a relatively dense matrix structure. However, prominent cracks are observable at the adhesive interface with the cement mortar substrate. This observation is consistent with the mechanical property results for the reference group, which exhibited higher compressive strength but lower tensile and adhesive strengths. In contrast, the inter-facial transition zones between X0.4/V6 series and the cement-based substrate exhibited a more continuous and compact structure compared to the reference group, with no obvious cracks observed. This explains why the adhesive strengths of X0.4 and V6 were higher than that of the reference group.



(**a**) Flexural strength (**b**) Compressive strength

(**c**) Tensile Strength (**d**) Adhesive strength

Figure 12. Mechanical properties of GP mortar specimens in different curing conditions.



(**a**) reference (0) (**b**) X0.4

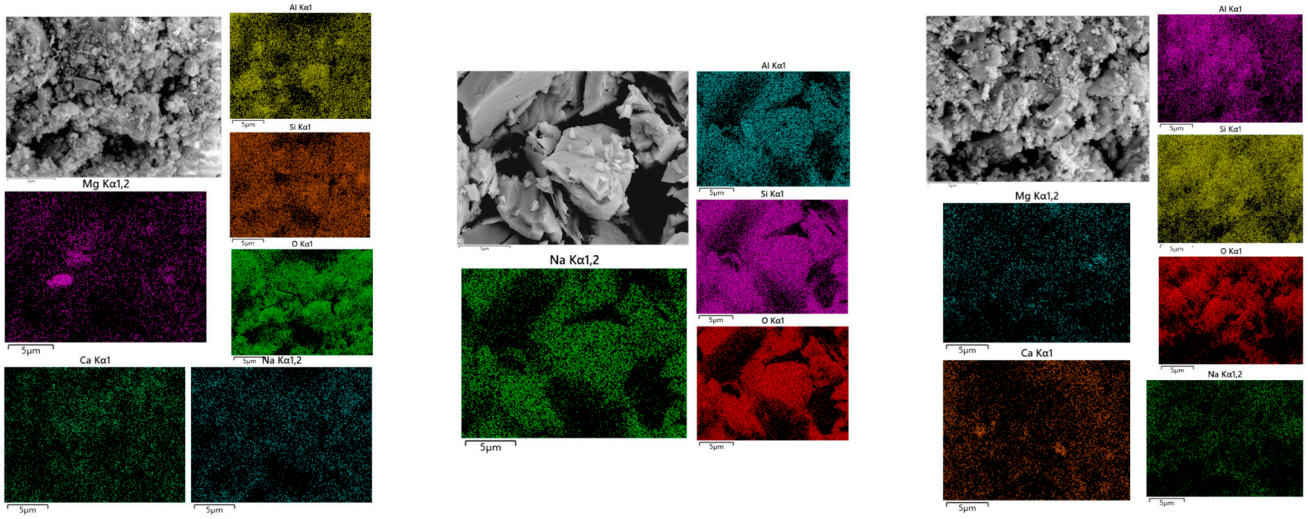
(**c**) V6 × 2000 (**d**) V6 × 10,000

Figure 13. SEM micrographs for reference (0), X0.4 and V6 samples.

Further examination of the V6 sample via high-magnification SEM (Figure 13d) indicated that its interfacial surface was covered by continuous film-like material. This polymer film, derived from the VAE emulsion, enhances interfacial adhesion through two primary mechanisms: first, by forming a physical bridge across microcracks in the matrix, and second, through chemical bonding between hydroxyl (-OH) groups in the polymer and hydration products of the cementitious substrate [41,42].

However, while the polymer film improves adhesion, it also introduces a "soft interlayer effect," which restricts the extent to which compressive strength can be improved in the GP mortar [34,43]. As revealed in Figure 13c, the V6 mortar exhibits a looser and more porous microstructure compared to the X0.4 and reference samples. The structure contains multiple irregular cracks and a greater proportion of unreacted material, which can be attributed to the retardation of geopolymerization and hydration reactions by VAE. The delayed reaction kinetics result in incomplete reaction progression and a higher content of unreacted precursors in the hardened matrix.

According to the mapping diagrams of the three samples (Figure 14), more Na, Al, Si and O substances (presumably N-A-S-H gel) were generated in X0.4 sample (with 0.4% HPMC), while the signal of calcium containing substances was weak and could not be clearly shown in the spectrum. The enhanced formation of N-A-S-H with HPMC addition is linked to its high sodium sulfate content. The XRD results confirm this enhancement, which is consistent with established findings that sodium sulfate promotes N-A-S-H gel formation, by providing additional sodium ions [44].



(**a**) reference (0) (**b**) X0.4 (**c**) V6

Figure 14. EDS mapping images of reference (0), X0.4 and V6 samples.

3.5. XRD Analysis

The XRD patterns of X0.4, V6, and reference group samples after 28 days of curing are shown in Figure 15. The results indicate that, compared to the reference group without additives, the diffraction peaks of amorphous silica and C-S-H gel in X0.4 and V6 samples were significantly weakened. The increase in sodium aluminium silica is more pronounced in the X0.4 samples' XRD pattern. Combined with the mapping results, it is speculated that the sodium aluminium silica is N-A-S-H gel [45]. These microstructural changes explain why the durability of the X0.4 specimen is higher compared to the reference group and V6. Additionally, mullite and unreacted calcium silicate (C-S) phases were observed in the XRD spectra of the X0.4 and V6 samples. The presence of unreacted phases confirms the delayed

hydration process of geopolymers due to the addition of HPMC and VAE, consistent with mechanical, durability, and SEM observations.

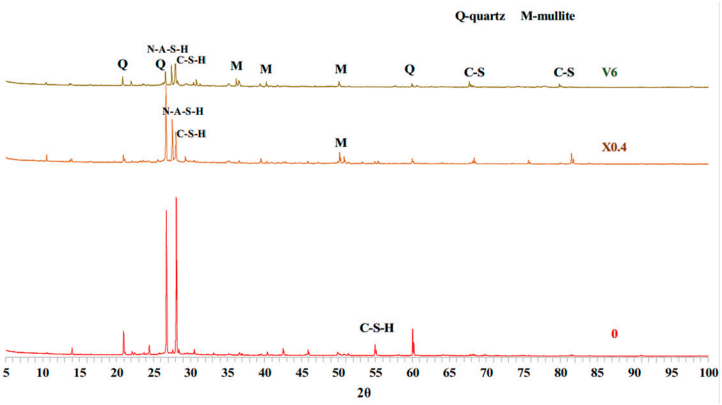


Figure 15. XRD patterns for reference (0), X0.4 and V6 samples.

The action mechanisms of VAE and HPMC diverge fundamentally, with the former exerting chemical inhibition and the latter providing physical and physicochemical enhancement. For VAE, the mechanism involves the alkaline hydrolysis of acetate ester groups, releasing CH_3COO^- ions that sequester Ca^{2+} to form calcium acetate [46]. This consumption of calcium ions disrupts the ionic equilibrium, ultimately suppressing the nucleation and growth of C-S-H gel [46]. In contrast, HPMC enhances the system through multiple complementary pathways. It acts as a physical barrier by adsorbing onto particle surfaces, delaying the dissolution reaction. Its excellent water-retaining property enables internal curing, promoting prolonged hydration and later-age strength gain [47]. Additionally, the incorporated air bubbles improve workability and facilitate the formation of a denser microstructure, which collectively boosts mechanical performance and durability.

4. Conclusions

This study systematically investigates the effects of HPMC and VAE polymers on the properties of geopolymer (GP) mortar based on industrial solid waste. The results indicate that both polymers enhance the adhesive strength of the mortar, though their overall influences are contrasting. An optimal HPMC content (0.4%) improves compressive strength and refines the microstructure by virtue of its water-retaining capacity, whereas excessive incorporation leads to air entrainment and reduced matrix density, thereby diminishing flexural and splitting tensile strengths. In contrast, the addition of VAE markedly increases splitting tensile and adhesive strength—reaching a peak adhesion of 1.79 MPa at 6% dosage, despite progressively reducing compressive and flexural properties. Microstructural analysis reveals that VAE consumption of OH^- and Ca^{2+} inhibits geopolymerization and C-S-H gel formation, resulting in higher porosity. Nevertheless, the in situ-formed polymer films act as effective bridges between reaction products and enhance interfacial bonding, which explains the improved adhesion. In terms of durability, HPMC significantly strengthens resistance to water, acid, and high-temperature exposure, while VAE exerts a negative impact. Furthermore, sealed curing is demonstrated to be a viable alternative to standard curing, offering equivalent performance.

In light of these complementary characteristics, future research should aim to develop an integrated HPMC-VAE system to synergistically enhance the overall performance of geopolymer mortar.

Author Contributions: Conceptualization, W.J. and S.L.; validation, B.S. and M.C.; formal analysis, S.L. and P.C.; investigation, P.C. and Z.Z.; resources, H.Y. and S.L.; data curation, P.C. and Z.Z.; writing—original draft preparation, P.C. and Z.Z.; writing—review and editing, S.L.; supervision, Y.L. and H.Y.; project administration, M.C. and S.L.; funding acquisition, W.J. and Y.L. All authors have read and agreed to the published version of the manuscript.

Funding: This work was financially supported by Hebei Province Department of Education Fund (QN2025425), Hebei Province Foundation for Returned Scholars (C20220320), Dr. startup funds (1181389), and Sub project of China Construction Engineering Corporation's Technology Research and Development Project (CSCEC-PT-015-203).

Data Availability Statement: The data presented in this study are available on request from the corresponding author.

Conflicts of Interest: Author Wenjun Ji, Ying Lu, Baolong Shan, Mengyan Chi was employed by the company China Construction First Group Decoration Corporation Limited. The remaining authors declare that the research was conducted in the absence of any commercial or financial relationships that could be construed as a potential conflict of interest.

References

1. Majhi, R.; Nayak, A.; Mukharjee, B. Characterization of lime activated recycled aggregate concrete with high-volume ground granulated blast furnace slag. *Constr. Build. Mater.* **2020**, *259*, 119882. [CrossRef]
2. Liu, Z.; Cheng, G.D.; Huang, T.Y.; Wang, D.M. Study on properties of fly ash-slag based geopolymer mortar. *Bull. Chin. Ceram. Soc.* **2019**, *38*, 1883–1888.
3. Cao, L.; Zhang, H.Y.; Wu, B. Study on shear behavior of reinforced concrete beams strengthened with textile-reinforced geopolymer mortar. *J. Eng. Mech.* **2019**, *36*, 207–215.
4. Cao, X.Y.; Yang, J.S. Overview of cementitious properties of geopolymer mortar and its concrete. *Bull. Chin. Ceram. Soc.* **2019**, *38*, 1–9.
5. Yin, Y.L. Study on Mechanical Properties and Durability of Basalt Fiber Concrete. Master's Thesis, Chongqing Jiaotong University, Chongqing, China, 2015.
6. Jia, Y.H. Preparation and Performance of Na-Fly Ash Geopolymer. Ph.D. Thesis, China University of Mining and Technology, Beijing, China, 2009.
7. Ohama, Y. Polymer-based admixtures. *Cem. Concr. Res.* **1998**, *20*, 189–212. [CrossRef]
8. Ou, Z.H.; Ma, B.G.; Jian, S.W.; Shen, Y.H. Influence of cellulose ether molecular parameters on mechanical properties of cement paste. *Bull. Chin. Ceram. Soc.* **2016**, *35*, 2371–2377.
9. Feng, K.; Ma, K.; Wang, J.; Long, G.; Xie, Y.; Zeng, X.; Tang, Z.; Usman, I.U. Influence of cellulose ethers on rheological properties of cementitious materials: A review. *J. Build. Eng.* **2024**, *95*, 110347. [CrossRef]
10. Pourchez, J.; Grosseau, P.; Ruot, B. Changes in C3S hydration in the presence of cellulose ethers. *Cem. Concr. Res.* **2010**, *40*, 179–188. [CrossRef]
11. Yang, K. Research on Formula Optimization of Self-Compacting Concrete Admixtures. Master's Thesis, Guizhou University, Guiyang, China, 2024.
12. Brachaczek, W. Influence of Cellulose Ethers on the Consistency, Water Retention and Adhesion of Renovating Plasters. *IOP Conf. Ser. Mater. Sci. Eng.* **2019**, *471*, 032020. [CrossRef]
13. Batista, I.L.R.; Cabral, K.C.; de Souza, W.R.M.; Fontes, A.É.M.d.S.; Martinelli, A.E. Influence of hydroxypropylmethylcellulose (HPMC) on thermal and mechanical performance of cementitious rendering mortars. *Mater. Struct.* **2024**, *57*, 25. [CrossRef]
14. Wang, P.M.; Zhao, G.R.; Zhang, G.F. Action mechanism of redispersible polymer powder in cement mortar. *J. Chin. Ceram. Soc.* **2018**, *46*, 256–262.
15. Luo, J.J.; Zhang, L.L.; Liu, Y.X.; Man, L.Y. Comparative study on properties of cement-based pervious concrete modified by redispersible latex powder and silica fume. *Concr. Cem. Prod.* **2018**, *12*, 23–26.
16. Qiao, Q.; Chai, H.C.; Zhang, X.T.; Zhang, H.B. Study on redispersible latex powder modified cement-based thin spray materials. *Bull. Chin. Ceram. Soc.* **2022**, *41*, 3394–3402.
17. Li, J.H.; Zhao, W.J. Research progress on redispersible latex powder. *Bull. Chin. Ceram. Soc.* **2016**, *35*, 4038–4043.
18. Zhang, J.; Bian, C.; Chen, B.; Li, C.; Wei, H.; Lu, H. Study on the Mechanical Properties, Tensile Performance, Hydration Heat, and Microstructure of VAE-Modified Rubber Mortar. *Materials* **2025**, *18*, 651. [CrossRef] [PubMed]

19. Cheng, J.; Shi, X.; Xu, L.; Zhang, P.; Zhu, Z.; Lu, S.; Yan, L. Investigation of the Effects of Styrene Acrylate Emulsion and Vinyl Acetate Ethylene Copolymer Emulsion on the Performance and Microstructure of Mortar. *J. Build. Eng.* **2023**, *75*, 106965. [CrossRef]
20. Meng, L.N.; Liang, J.F.; Chen, L. Study on mechanical properties of recycled powder-redispersible latex powder composite cement mortar. *Concrete* **2023**, *2*, 129–135.
21. Peng, J.H.; Mao, J.B.; Zhang, J.X.; Qu, J.D.; Teng, C. Modification effect of redispersible latex powder on cement mortar. *Bull. Chin. Ceram. Soc.* **2011**, *30*, 915–919.
22. Qiao, J.L.; Liu, B.; Ma, L.G.; Li, S.Y.; Ju, X.T. Experimental study on working performance of modified high-performance polymer cement mortar. *Concrete* **2022**, *1*, 149–152.
23. Wang, H.; Zhu, Y.; Li, T.; Li, X.; Peng, S.; Guo, J.; Pei, X.; Zhong, C.; Yang, Y.; Ma, Q.; et al. Modification Mechanism of Low-Dosage Vinyl Acetate-Ethylene on Ordinary Portland Cement-Sulfoaluminate Cement Binary Blended Rapid Repair Mortar. *Polymers* **2025**, *17*, 1501. [CrossRef] [PubMed]
24. Xing, C.W. Study on adhesive strength and Durability of Geopolymer Mortar. Master's Thesis, Hebei University of Science and Technology, Shijiazhuang, China, 2022.
25. *JC/T 547-2017*; Ceramic Tile Adhesives. China Architecture & Building Press: Beijing, China, 2017.
26. *GB/T 1346-2024*; Test Methods for Water Requirement of Normal Consistency, Setting Time and Soundness of the Portland Cement. China Architecture & Building Press: Beijing, China, 2024.
27. *GB/T 2419-2005*; Test Method for Fluidity of Cement Mortar. China Architecture & Building Press: Beijing, China, 2005.
28. *GB/T 17671-2021*; Test Method of Cement Mortar Strength (ISO Method). China Architecture & Building Press: Beijing, China, 2021.
29. *GB/T 29417-2012*; Test Methods for Drying Shrinkage Stress and Cracking Possibility of Cement Mortar and Concrete. China Architecture & Building Press: Beijing, China, 2012.
30. *JGJ/T 70-2009*; Standard for Test Method of Basic Properties of Construction Mortar. China Architecture & Building Press: Beijing, China, 2009.
31. *GB/T 50082-2024*; Standard for Testing Methods for Long-Term Performance and Durability of Concrete. China Architecture & Building Press: Beijing, China, 2024.
32. Yue, P.; Wang, L.L. Interfacial temperature of EPS external wall insulation system in high temperature environment in summer. *Urban. Archit.* **2019**, *16*, 96–99.
33. Chi, L.; Yanmin, J. Effect of Redispersible Latex Powder and Fly Ash on Properties of Mortar. *Coatings* **2022**, *12*, 1930. [CrossRef]
34. Wang, X.L.; Feng, H.C.; Zhou, K. Mix ratio optimization and frost resistance of VAE latex powder modified cement mortar. *Bull. Chin. Ceram. Soc.* **2023**, *42*, 3462–3469.
35. Huang, Y.C.; Zhang, Y.M. Effect of emulsion compounding on polymer cement waterproof coating film in tile adhesive system. *Mater. Rep.* **2022**, *36*, 572–577.
36. Shi, X.; Ning, B.; Na, F.; Zhao, W.; Zhang, C. Study on properties of re-dispersible latex powder and polypropylene fiber-reinforced lightweight foam concrete. *J. Build. Eng.* **2024**, *95*, 110156. [CrossRef]
37. Wang, Z.H.; Bai, E.L.; Zhou, J.P.; Liu, G.J.; Yang, N. Mechanical properties of VAE latex powder/carbon fiber composite modified concrete. *J. Build. Mater.* **2024**, *27*, 487–495.
38. Zhang, N.; Sun, Q.; Zhang, P.Y.; Wang, D.M.; Wang, Q. Effects of Polymers on Waterproofing and Mechanical Properties of Mortar after Heat Treatment. *Bull. Chin. Ceram. Soc.* **2023**, *42*, 2703.
39. Lau, C.K. Investigation on Alkali Activated Materials: Materials to Structures. Ph.D. Thesis, Curtin University, Perth, Australia, 2021.
40. *JG/T 287-2013*; The Materials of External Thermal Insulation Systems Basedon Insulated Decorative Panel. China Architecture & Building Press: Beijing, China, 2013.
41. Shi, X.; Xu, L.L.; Feng, T.; Han, J.; Zhang, P. Research progress on waterborne polymer emulsion modified cement mortar. *Bull. Chin. Ceram. Soc.* **2021**, *40*, 2497–2507.
42. Yan, S.; Lu, H.; Zhou, Z.; Dong, Q.; Chen, X.; Wang, X. A polymer latex modified superfine cement grouting material for cement-stabilized macadam: Experimental and simulation study. *Constr. Build. Mater.* **2024**, *413*, 134893. [CrossRef]
43. Han, D.D.; Chen, W.D.; Zhong, S.Y. Effect of latex particle size on properties of polymer-modified cement-based materials. *J. Build. Mater.* **2017**, *20*, 943–949.
44. Lv, Q.-F.; Wang, Z.-S.; Gu, L.-Y.; Chen, Y.; Shan, X.-K. Effect of sodium sulfate on strength and microstructure of alkali-activated fly ash based geopolymer. *J. Cent. South Univ.* **2020**, *27*, 1691–1702. [CrossRef]
45. Song, K.-I.; Song, J.-K. Carbonation characteristics of alkali-activated blast-furnace slag mortar. *Adv. Mater. Sci. Eng.* **2014**, *2014*, 326457. [CrossRef]

46. Zhang, G.F.; Wang, P.M.; Zhao, G.R. Calorimetric study on the influence of redispersible E/VC/VL terpolymer on the early hydration of Portland cement. *J. Therm. Anal. Calorim.* **2016**, *124*, 1229–1241. [CrossRef]
47. Li, L.; Wang, Y.; Ma, Y.Y.; Shen, H.Q.; Luo, J.H. Study on thermal conductivity and pore structure of foamed concrete based on orthogonal test. *Bull. Chin. Ceram. Soc.* **2024**, *43*, 2888–2896.

Disclaimer/Publisher's Note: The statements, opinions and data contained in all publications are solely those of the individual author(s) and contributor(s) and not of MDPI and/or the editor(s). MDPI and/or the editor(s) disclaim responsibility for any injury to people or property resulting from any ideas, methods, instructions or products referred to in the content.